

We are IntechOpen, the world's leading publisher of Open Access books Built by scientists, for scientists

5,800

Open access books available

142,000

International authors and editors

180M

Downloads

Our authors are among the

154

Countries delivered to

TOP 1%

most cited scientists

12.2%

Contributors from top 500 universities



WEB OF SCIENCE™

Selection of our books indexed in the Book Citation Index
in Web of Science™ Core Collection (BKCI)

Interested in publishing with us?
Contact book.department@intechopen.com

Numbers displayed above are based on latest data collected.
For more information visit www.intechopen.com



Chapter

Green and Sustainable Chemical Looping Plasma Process for Ammonia and Hydrogen Production

Mohsen Sarafraz, Farid Christo and Bernard Rolfe

Abstract

The overarching aim of this chapter is to propose a novel clean thermochemical process that harnesses thermal plasma technology to co-produce hydrogen and ammonia using a chemical looping process. The thermodynamic potential and feasibility of the process were demonstrated using a simulation of the system with aluminium and aluminium oxide as the oxygen and nitrogen carriers between the reactors. The effect of different operating parameters, such as feed ratio and temperature of the reactor, on the energetic performance of the process was investigated. Results showed that the nitridation and ammoniation reactors could operate at < 1000 K, while the thermal plasma reactor could operate at much higher temperatures such as (> 6273 K) to reduce the alumina oxide to aluminium. The ratio of steam to aluminium nitride was identified as the key operating parameter for controlling the ammoniation reactor. Using a heat recovery unit, the extracted heat from the products was utilised to generate auxiliary steam for a combined cycle aiming at generating electricity for a thermal plasma reactor. It was demonstrated that the process can operate at an approximate self-sustaining factor ~ 0.11 , and an exergy partitioning fraction of up to 0.65. Integrating the process with solar photovoltaic showed a solar share of $\sim 32\%$ without considering any battery storage units.

Keywords: three-stage chemical looping, ammonia, hydrogen, aluminium oxide, thermal plasma

1. Introduction

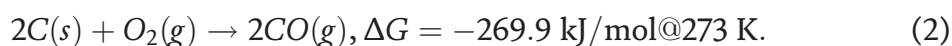
Ammonia is a key hydrogen carrier with the potential to be utilised as a fuel, an intermediate product, and also a combo product (of hydrogen and nitrogen) for agricultural and pharmaceutical applications. The current chemical pathway for generating ammonia is through the Haber-Bosch (HB) methane reforming process [1, 2] which is highly dependent on the quality and price of natural gas. The Haber-Bosch process includes consecutive stages of methane reforming, followed by water-gas shift improvement and catalytic nitrogen fixation at high pressure and low temperatures

[3, 4]. All these stages are energy-intensive, far from equilibrium and release CO₂ as part of the process due to the number of reformers existing in the process [5]. Hence, the HB process is not a sustainable cycle for nitrogen fixation [6] and ammonia production considering the technical challenges associated with environmental pollution and global warming [7].

The main issue with CO₂ formation is the presence and adjacency of oxygen and carbon that can generate either CO₂ via complete combustion, or CO through partial oxidation reactions as represented below:



and



Reactions 1 and 2 can proceed depending on the availability of the oxygen in the reactor, referred to as the “O/C” molar ratio. In conventional combustors and gaseous reactors, these reactions will always occur due to the direct contact of oxygen and carbon. Therefore, new combustion systems should be developed to avoid the production of Green House Gases (GHGs). Chemical looping technology [8] is a promising thermochemical pathway by which the direct contact between air and fuel is inherently hindered, thereby avoiding the production of CO₂ and/or CO. In a chemical looping system, oxygen is transported between two reactors via an oxygen carrier (OC), which has the following properties:

- An oxygen carrier should provide sufficient oxygen content and reduction–oxidation capacity (cyclic redox) [9–11]. This means that the oxygen carrier should be able to release the oxygen where required and absorb it using a cyclic process for an unlimited time while retaining its solid physical properties, morphology, and structure [11, 12].
- The oxygen carrier should have suitable thermophysical properties such as high thermal conductivity, high heat capacity and density, hence representing favourable thermal diffusivity, $(\frac{k}{\rho c})$ [13]. It is a key thermal characteristic that affects the residence time of the oxygen carrier in the reduction and/or oxidation reactors. It will also promote thermal performance and heat transfer coefficient in the reactor [14].
- The oxygen carrier should also offer various stable states of oxidation [15]. Accordingly, depending on the operating conditions, end-user requirements and products, the chemical pathway can be designed based on these stable oxidation states.

A general chemical looping system includes reactors (for combustion [16], reforming [17], or gasification [18]) or as will be investigated here, it has three reactors (for ammonia/hydrogen production) [19] in which cyclic reduction and oxidation occurs.

There has been extensive research conducted on the potential of chemical looping systems for hydrogen production. For example, steam chemical looping gasification [20] or CO₂-chemical looping gasification [21, 22] is one potential configuration that

has been extensively investigated for H₂-enrich fuel production. For example, He et al. [23] recently, proposed a new concept for steam chemical looping gasification to decrease the exergy destruction and to improve the cold gas efficiency of the gasifier. They used coal as the source of fuel and demonstrated that the efficiency of the cold gas can be as high as 86% in a three-stage chemical looping system. Also, the energy efficiency of 62.3% was calculated for the proposed plant. Pan et al. [24] used industrial waste such as gypsum and steel slag as the oxygen carrier to operate a steam chemical looping gasification system for generating H₂-enriched fuel. Based on the FactSage calculation [25] and experimental validation, they found that the optimum temperature for the gasification is around 1023 K, with a feedstock/oxygen carrier ratio of 1 and steam to oxygen carrier of 0.6. In a similar study, Zhao et al. [26] assessed a novel chemical looping gasification concept in which NiFe₂O₄ and CuFe₂O₄ particles were synthesised and utilised as an oxygen carrier for hydrogen production. They identified the optimum operating conditions for both reduction and oxidation reactions and showed that the gas yield can be as high as 64.98 mol/kg and syngas quality can reach 2.79 which is suitable for gas to liquid and Fischer-Tropsch processes [27, 28].

CO₂-chemical looping gasification is another process similar to dry gasification or pyrolysis which is used to generate syngas from coal or biomass. Recently, Xu et al. [22] developed thermodynamic models followed by conducting a series of experiments to assess the gasification of rice husk char sourced from pellet pyrolysis. They investigated the effect of various operating parameters including temperature, CO₂ concentration, and quantity of the oxygen carrier on the performance of the system. They showed that the presence of CO₂ can influence the performance of the gasification process. Also, they identified a mass transfer resistance within the char particles due to the change in the pore structure of the feedstock, which affected the gasification conversion. Zhang et al. [29] evaluated the effect of the red mud as the active oxygen carrier on the pyrolysis and gasification in a chemical looping gasification process. They utilised a fluidised bed reactor and investigated the effect of temperature (750–900°C) and also the ratio of the oxygen carrier to fuel (0.1–0.7) on the syngas quality and chemical conversion extent of the fuel. The results indicate that red mud promoted the pyrolysis reaction and also intensified the gasification reaction. However, increasing the temperature decreased the syngas quality from 7.26 to 4.83. In another study, Zhang et al. investigated a novel hydrogen production process with integration of CaO - Ca(OH)₂ thermal storage unit for gasification of coal and biomass using chemical looping of calcium. The thermal storage unit decreased the quantity of oxygen carrier required for the process and also improved the rate of hydrogen production. At optimum conditions of temperature and pressure, the gas yield was 17% higher than a normal process. The process was reported to have an energy conversion efficiency of 42.1% together with an exergy efficiency of 39.4%.

Figure 1 represents schematic diagrams of two-stage and three-stage chemical looping technologies. In a three-stage chemical looping, it is assumed that the third reactor can dissociate the metal oxide into reduced metal directly and without any side reaction with air or other chemicals. However, in the two-stage chemical looping, the second reactor requires air to regenerate the oxygen content of the oxygen carrier.

As represented in **Figure 1a**, for combustion/gasification chemical looping systems, a reduction reaction occurs, in the fuel reactor between a metal oxide and a fuel, which is an endothermic reaction requiring an external energy resource to drive the reaction to its equilibrium. For example, for alumina oxide as an oxygen carrier in a

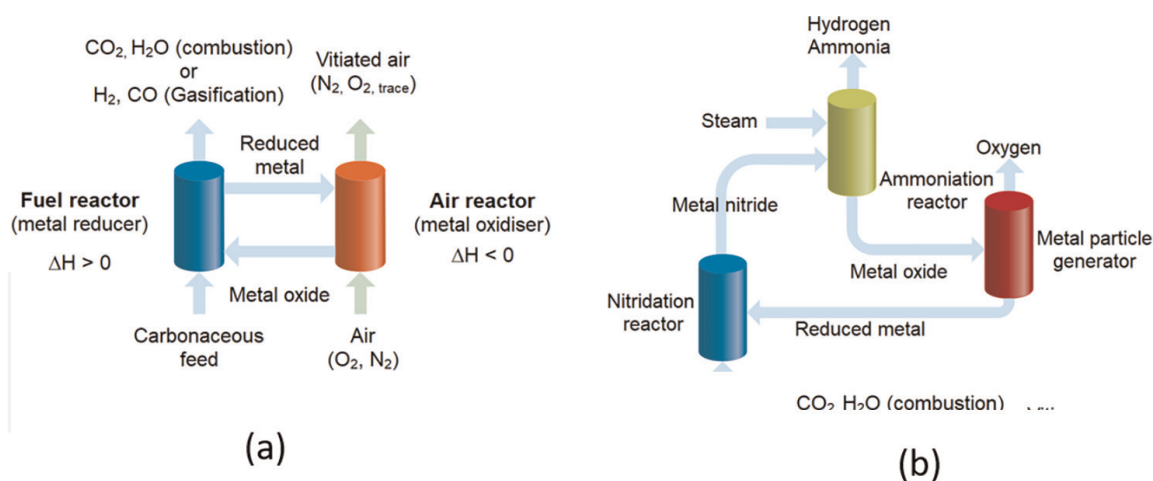
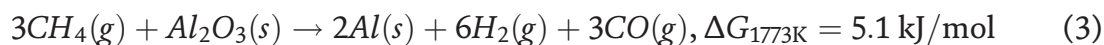
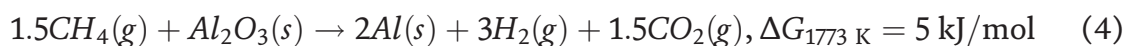


Figure 1. Chemical looping systems for a) two-stage reforming/combustion/gasification and b) three-stage ammonia/hydrogen production.

chemical looping reforming system for CH_4 , in the fuel reactor, methane reacts with aluminium oxide according to the following reaction:



or



The Gibbs value (ΔG) of both reactions are relatively the same. Hence, to determine the dominant reaction in the fuel reactor, the thermodynamic condition of the reactor must be studied, which includes the operating temperature and pressure of the fuel reactor, and the quantity of Al/aluminium oxide (oxygen availability, i.e., the O/C ratio). In the air reactor, the reduced metal (Al for our reactor) reacts with an abundant amount of air via an exothermic reaction to generate aluminium oxide particles and vitiated air. The vitiated air can then be utilised for electricity generation via gas combined power cycles, while the re-generated metal oxides can be fed into the fuel reactor again to be reduced over reforming reaction. As shown in the literature review section, it was identified that chemical looping gasification (either with steam or CO_2) is mainly used for generating syngas fuel. Accordingly, gasification includes the emission of CO_2 and CO as the products of the process. However, in the present work, the chemical looping technology will be utilised to generate hydrogen and ammonia instead of hydrogen and carbon monoxide, thereby either reducing or eliminating the carbon footprint from the process.

With process modifications, as represented in **Figure 1b**, the chemical looping technology can be utilised for the co-production of ammonia and hydrogen referred to as “3-stage chemical looping ammonia production, 3CLAP”. In the nitridation reactor, a metal nitride can be formed by a direct exothermic reaction between a metal and a pure nitrogen stream. Pure nitrogen steam can be sourced from an air separation unit or any vitiated air from other industrial processes that have 99% nitrogen purity. In the ammoniation reaction, the metal nitride reacts with steam to generate ammonia and/or hydrogen depending on the availability of the steam, temperature of the reaction, and quantity of metal nitride in the reactor. The metal oxide produced from the ammoniation reactor is then fed into a dissociation reactor to be dissociated into

pure metal and oxygen. While metal is fed into the nitridation reactor, oxygen can be chilled, stored and used for other industrial/health applications.

The main bottleneck of the 3CLAP system is the dissociation reactor. This is because dissociating metal oxides, such as Al_2O_3 , requires high temperatures ($\sim 6273\text{ K}$) to provide sufficient thermal driving force for such a highly positive Gibbs free energy of the “metal oxide to reduced metal reaction”. Such high temperatures cannot be maintained by conventional reactors; hence, thermal plasma is suggested as a potential technology that can be utilised in this process.

In this chapter, the use of thermal plasma technology as a disruptive method is proposed to push the boundaries of dissociation reactors, and increase the chemical efficiency and performance of the process. Also, a renewable energy-friendly concept has been designed and simulated to demonstrate the feasibility of co-production of hydrogen and ammonia when integrated with photovoltaic solar energy generation. For the proposed process, Al/ Al_2O_3 pair was used as it has reasonably large Gibbs free energy and a tendency to participate in the reaction, favourable thermophysical properties and stable thermodynamic phases during cyclic reduction and oxidation reactions. The Gibbs minimisation method coupled with thermochemical analysis was utilised to quantify the thermodynamic performance of the proposed system including hydrogen/ammonia ratio, exergy partitioned in the gas products, 1st law thermodynamic efficiency, self-sustaining factor, exergy partitioning factor, and renewable energy share (solar share).

2. Conceptual design of 3CLAP and its configuration

2.1 Process design

Figure 2 represents a detailed illustration of a three-stage chemical looping ammonia production system [19] designed for integration with a photovoltaic solar farm. In this process, three reactors for nitridation, ammoniation and thermal plasma

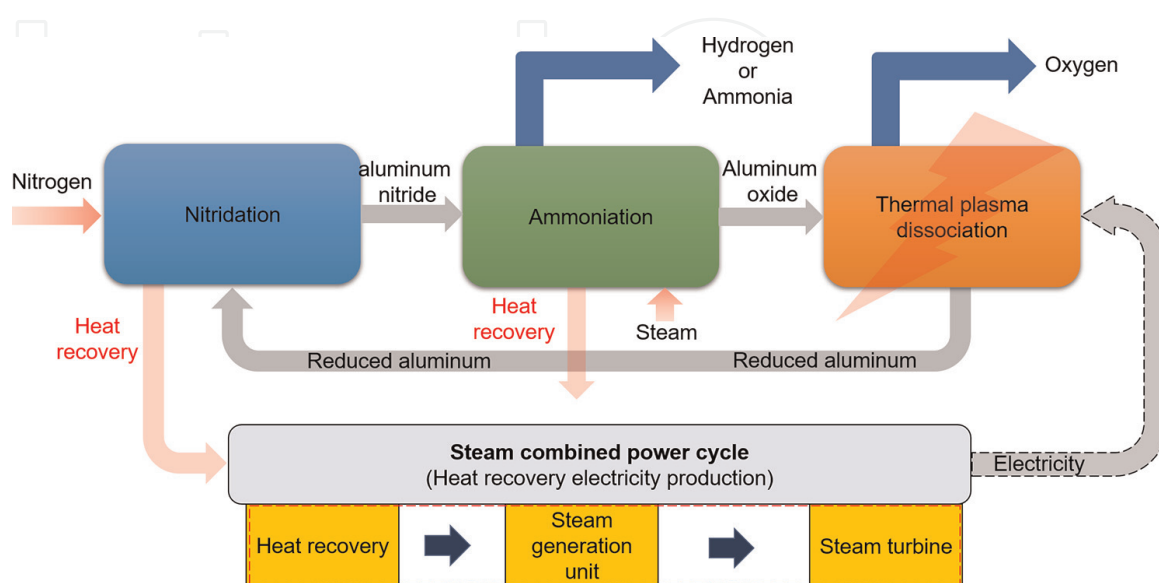


Figure 2.
An illustration of the proposed process for hydrogen and ammonia production using the aluminium chemical looping process.

are utilised amongst which thermal plasma is integrated with solar PV, while a heat recovery system is designed to recover heat from the reactors' outlets.

As already discussed, the energy of the thermal plasma is proposed to be supplied from renewable energy sources, such as solar photovoltaic combined with the electricity that can be generated from a built-in power cycle (steam combined cycle from the recovered heat of the processes), thereby improving the process sustainability and its energetic performance.

Figure 3 shows the process model developed using the Aspen Plus software package for simulating the 3CLAP process operating with alumina. Alumina was selected because it has high thermal conductivity, good thermal response, and high Gibbs free energy. Also, in the model, the aluminium/aluminium oxide pair was assumed to remain solid in all process stages. Also, the separators were assumed to have 100% separation efficiency and a capacity to separate solid materials from gases. The steam flow rate in the steam power cycle was varied depending on the thermal loading of the heat recovery thereby enabling the steam turbine to operate at a constant stream inlet temperature.

The simulations were performed with the Aspen Plus software package coupled with Matlab and Homer [30–32] to simulate the photovoltaic panels. To simulate the reactors, the Gibbs minimisation method [33] was utilised for the nitridation, ammoniation, and thermal plasma reactors. Also, thermochemical equilibrium analysis [34] was used to conduct sensitivity analysis of the reactors against operating parameters such as temperature or feed ratios. All Gibbs's free energy parameters, enthalpy of reactions, and thermodynamic properties were extracted from Barin's Handbook [35]. In addition, the following assumptions were considered in the model:

1. No heat loss occurs from any reactors during the process which represents an ideal operating condition;
2. All reactions proceed to equilibrium as there is no impurity in the system;
3. As the temperature is below the melting point, no structural change and morphology change occurs in the solid phase;
4. There is a robust particle handling system available to feed the particles in and from the reactors;

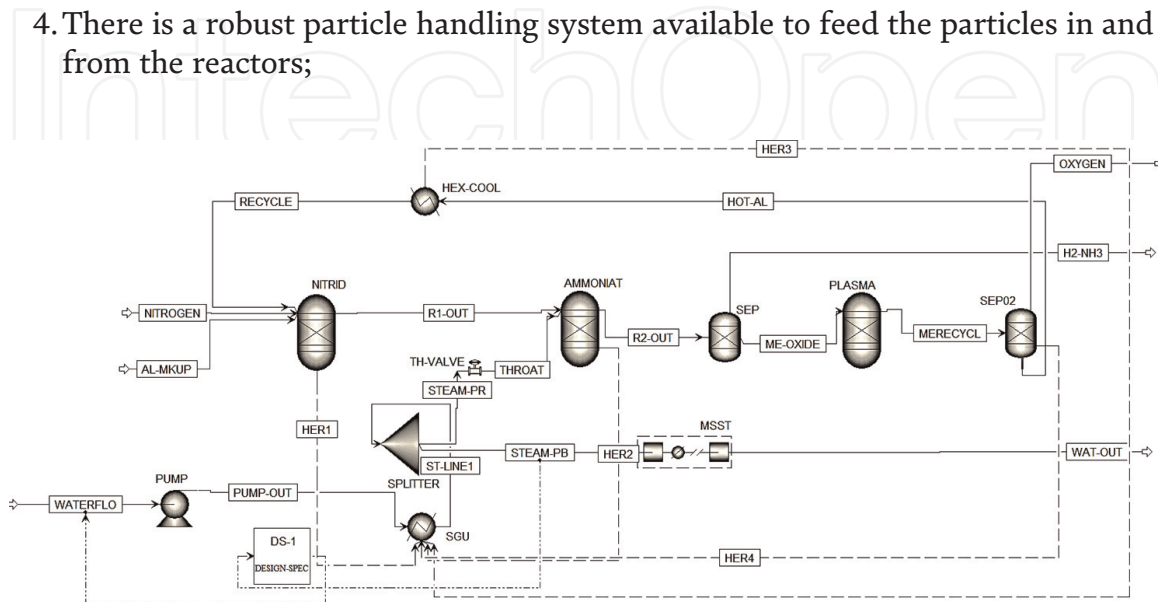


Figure 3. The Aspen plus model was developed for simulating the 3CLAP system.

5. There are no side reactions between the walls of the reactors, and the solid particles;
6. There is a rapid quenching system for the thermal plasma reactor to cool the particles once they are formed inside the reactor to avoid driving other side reactions.

These assumptions are used to simplify the analysis and provide a benchmark of an ideal process. However, in practice, an adjustment based on the specific design is required in the model to account for the effect of imperfections and non-ideal conditions on the physical performance of the system.

2.2 Aluminium-oxygen-nitrogen thermodynamic system

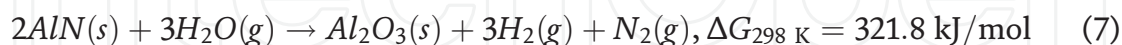
As a preliminary step, the change in the Gibbs free energy of each reaction must be evaluated at equilibrium conditions to ensure reactions are thermodynamically feasible in fuel or air reactors. Accordingly, to assess the thermodynamics of the 3CLAP system at equilibrium conditions, it is necessary to consider aluminium, nitrogen and oxygen and any oxidation states such as Al_2O_3 as part of the thermodynamic system. Since all reactors work at atmospheric pressure, the Gibbs minimisation analysis is assumed to be only a function of temperature. In the nitridation reactor, the following reaction occurs:



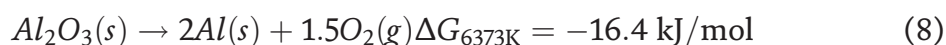
The AlN formed in the reactor is then fed into the ammoniation reactor in which the following reaction is expected to occur:



The key operating parameter here is the molar ratio of the reactants (steam/AlN ratio) which determines the final product of the reactor. Hence, depending on the availability of nitrogen and steam in the reactor, the following reaction can occur in the ammoniation reactor:



The produced Al_2O_3 particles from both reactions are then fed into the thermal plasma reactor to be dissociated to aluminium and oxygen according to the following reaction:



The pure aluminium is then returned to the nitridation reactor, completing the cycle, while oxygen can be chilled and stored for industrial and/or hygienic applications. This reaction is endothermic, thereby high energy is required in the thermal plasma reactor. Also, there is a need to utilise a rapid quenching system to be able to create aluminium particles in a plasma environment. The rapid quenching system must be robust, with a small response time close to that of a plasma reactor (i.e., microseconds to milliseconds). Considering the existing

utilisation of plasma reactors for carbon black particle production [36], and the maximum temperature that a plasma reactor can reach [37], an arc thermal plasma is proposed. Combined with electricity produced via renewable energy sources, it decreases the emission of CO₂ and carbon footprint to the environment. As shown in **Figure 4**, a comparison between the equilibrium mole percentages of gaseous products in the thermal plasma reactor before and after the quenching shows that a rapid quenching system can operate at $T > 6373$ K to avoid recombination of oxygen and alumina. As shown in **Figure 4b**, the stable thermodynamic components after rapid quenching are Al₂O₃ and Al, while before quenching, O(g), O₂(g) and various solid phases of alumina are the dominant products of the thermal plasma.

2.3 Calculation of the thermodynamic parameter

To calculate the Gibbs free energy of the reactions and the change in the enthalpy of the proposed reactions, the following equation was utilised:

$$\Delta G_{R_i} = \sum \Delta G_{pro.} - \sum \Delta G_{Rct.} \quad (9)$$

In this equation, G is the Gibbs free energy (kJ/mol), *pro* and *Rct* are acronyms for the products and reactants. If $\Delta G_{R_i} > 0$, it shows that the reaction is not thermodynamically feasible, while $\Delta G_{R_i} < 0$ shows that the reaction will proceed towards equilibrium without any thermodynamic barrier.

The same equation was utilised for the enthalpy of reaction, which is as follows:

$$\Delta H_{R_i} = \sum \Delta H_{pro.} - \sum \Delta H_{Rct.} \quad (10)$$

In this equation, H is the enthalpy of reaction (kJ/mol). $\Delta H_{R_i} > 0$ shows that the reaction is endothermic thereby requiring thermal energy to proceed to the equilibrium state. However, $\Delta H_{R_i} < 0$ simply shows that reaction is exothermic, thereby releasing thermal energy during the reaction.

The self-sustaining parameter is defined as the ratio of the energy recovered and produced by the power block to the energy demand from the thermal plasma reactor defined with the following equation:

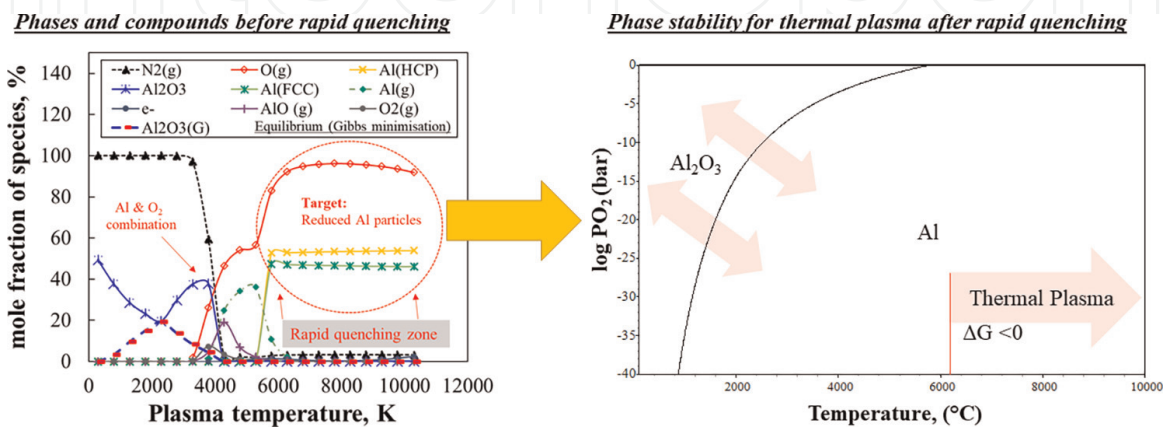


Figure 4. Formation and stability of different phases and compounds in the thermal plasma reactor before and after the rapid quenching process for metals and powders [38].

$$SSF = \frac{W_{Tur.}}{E_{TPR}} \quad (11)$$

In the above equation, $W_{Tur.}$ is the amount of energy recovered and converted to electricity using a multi-stage turbine from a built-in power block and E_{TPR} is the energy demand from a thermal plasma reactor.

The exergy partitioning factor is the amount of energy that can be stored in form of chemical exergy in the products of the plant and can be calculated using the following equation:

$$EPF = \frac{\dot{n}_{H_2}LHV_{H_2} + \dot{n}_{NH_3}LHV_{NH_3}}{\sum \Delta H_{net,reactors\ 1,2,3}} \quad (12)$$

Here, \dot{n}_i is the mole flow of component I, LHV is the acronym defined for the lower heat value for either hydrogen or NH_3 . The molar ratio of the steam to AlN is also defined as φ according to the following equation:

$$\varphi = \frac{[H_2O] \left(\frac{kmol}{h}\right)}{[AlN] \left(\frac{kmol}{h}\right)} \quad (13)$$

The above thermodynamic parameters were used in the calculations to assess the energetic performance and thermodynamic potential of the system.

3. Result and discussion

3.1 Nitridation reactor

Figure 5 represents the effect of temperature on the Gibbs free energy of the reaction in the nitridation reactor. As can be seen, by increasing the temperature of the reactor, for example from 250 K to 1000 K, the Gibbs free energy is decreased by ~25% recorded at atmospheric pressure. Also, the enthalpy of the reaction shows a

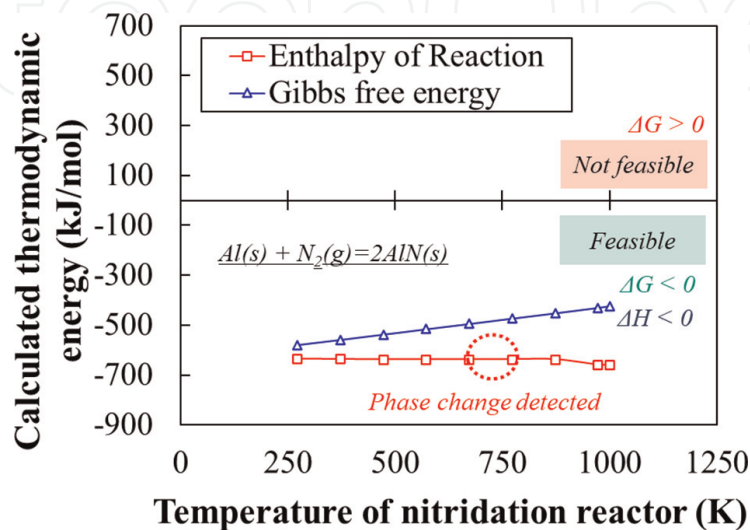


Figure 5. Variation of the Gibbs free energy and enthalpy of the reaction with the temperature of the nitridation reactor.

linear weak dependence on the temperature of the reactor because it is an exothermic reaction. For example, increasing the temperature from 250 K to 1000 K causes only a 1.4% decrease in the enthalpy of the reaction. Also observed, was a slight drop in the enthalpy around $T = 750$ K due to the phase change in the AlN (solid) to the eutectic and liquid phase. Notably, to avoid complexity in the operation and reduce potential plant costs associated with maintaining the operating pressure, all reactors are designed at atmospheric pressure. This is advantageous as it can reduce erosion and corrosion related to high-pressure gaseous reactions in the reactors. It is worth mentioning that reaction 5 is spontaneous, hence it is not energy-intensive and does not require a continuous energy source to maintain its temperature. It can proceed to equilibrium due to the heat released during the reaction. Also, considering the melting temperature of the aluminium, the operating temperature of the nitridation reactor is set to the minimum with a 50 K buffer zone to avoid any liquid metals and clogs forming inside the pipes and walls of the nitridation reactor. Thus, $T < 700$ K is designated as a suitable temperature for the operation of the reactor. These findings are in good agreement with the results obtained in the literature for the hydrolysis reactors. Wang et al. [39] showed that a similar reaction can be driven with a non-equilibrium hydrolysis reactor in a system referred to as “Chemical Looping Ammonia Generation” (CLAG).

3.2 Ammoniation reactor

The generated AlN from the nitridation reactor is fed into the ammoniation reactor to be blended and react with steam for ammonia generation. As already elaborated in Section 3, reactions 6 and/or 7 occurs in this reactor depending on the operating conditions and molar ratio of steam to AlN feed. As represented in **Figure 6**, the results of the equilibrium analysis for the ammoniation reactor showed that while the dominant reaction in the reactor is reaction 6, it is an exothermic reaction. Also, there is a weak dependence of the performance of the reactor on temperature. Also, the Gibbs free energy for the reactions showed that with an increase in the temperature of the reactor, the ΔG value increases by $\sim 30\%$.

For example, at $T = 900$ - 1000 K, -300 kJ/mol $< \Delta G < -400$ kJ/mol. This shows that the reaction is highly spontaneous in the reactor at this operating temperature

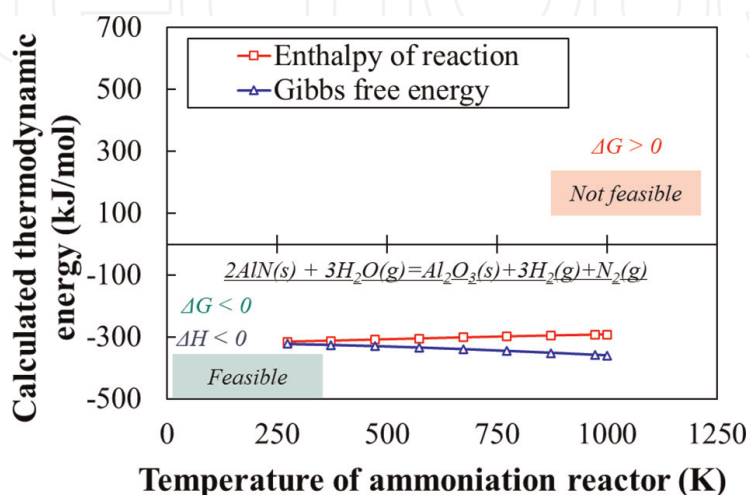


Figure 6. The variation of the Gibbs free energy and enthalpy of reaction with the temperature of the ammoniation reactor.

region while at any other operating temperature < 1000 K, the reaction is still feasible and can reach equilibrium without any phase change occurring inside the reactor. Hence, the temperature of the reactor must be chosen wisely to avoid phase change and melting in the reactor. Overall, the upper limit operating temperature for the reactor is ~ 1000 K in which particles are still solid, the Gibbs free energy is negative and the reaction is exothermic.

As shown in **Figure 7**, the molar ratio of steam/ AlN (φ value) is another key operating parameter that can control the chemical performance of the ammoniation reactor. Production rates of H_2 and NH_3 are nonlinearly dependent on the temperature of the ammoniation reactor, and it is proportional to the value of the steam to AlN ratio. For example, the final product from the ammoniation reactor could be determined by the φ value. As an example, at $T = 540$ K, for $0.5 < \varphi < 1$, the dominant product of the reactor is hydrogen with H_2/NH_3 ratio ~ 25 , while at $1 < \varphi < 3$, the H_2/NH_3 ratio significantly increases from 25 to 50 showing that production of ammonia is severely suppressed by increasing the amount of steam in the system. This is because, for larger φ values, the hydrogen and oxygen content in the reactor is increased which drives reaction 7 towards equilibrium. As a result, hydrogen production increases in the reactor. The best operating temperature range and φ values for producing hydrogen were at $T > 500$ K and $\varphi = 3$. While for ammonia production, not only the temperature of the reactor should be close to 300 K, but also the φ value should be below 0.5. The aluminium oxide produced in this reactor is then fed into the thermal plasma reactor to re-generate the reduced aluminium particles for completing the cycle and to provide the feed for the nitridation reactor. It is worth mentioning that in the hydrogen dominant operating region, still ammonia is produced, however, the mole fraction of the $\text{H}_2:\text{NH}_3$ is 1:300 or (less than 0.3%) that can be separated from the hydrogen stream using a robust aqua-ammonia condenser already developed in the literature [40] or hydrogen/ammonia membrane separators [41]. It is worth mentioning that alumina has already been identified as an oxygen carrier in a two-stage chemical looping ammonia production at 1773 K and 0.1 MPa using steam hydrolysis reaction. Galvez et al. [42] showed that both reactions can occur at atmospheric pressure without any added catalysts. They also advised that steam hydrolysis, which is an endothermic reaction, can be driven using concentrated solar thermal.

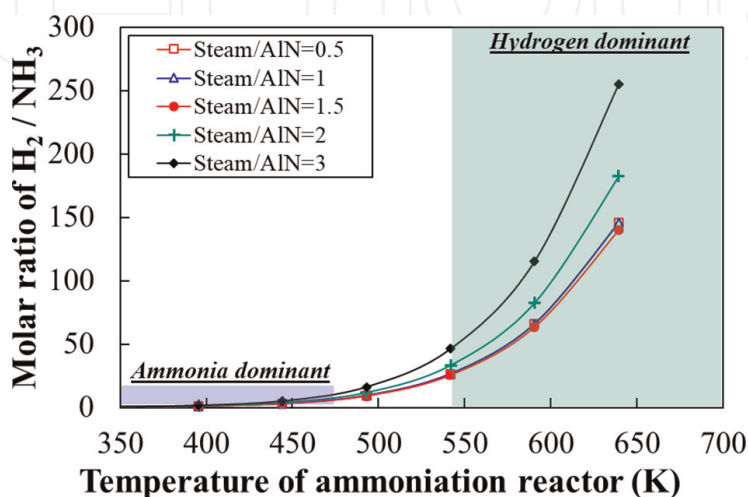


Figure 7. Variation of the H_2/NH_3 ratio with φ values at various operating temperatures inside the ammoniation reactor.

3.3 Thermal plasma reactor

In a plasma reactive system, the reactions are driven by a non-conventional energy source. A plasma stream includes (but is not limited to) ions, charged particles, neutral species, radicals, and spinning-vibrational excited species with relatively high Gibbs free energy ($-\Delta G$) that participate in the reaction. The bombardment of any neutral species by electrons (electron avalanche) and charged species in plasma can stimulate the material to aggressively participate in the reaction. A thermal plasma is a type of reactive plasma configuration in which reactions occur at very high temperatures typically in the range $6000 \text{ K} < T < 10,000$ (for example for arc plasma reactor). The high temperature of the plasma reactor ensures that the reactions can proceed to equilibrium, thereby reaching a high chemical conversion extent and chemical efficiency (generally $>99\%$). The results of the modelling for the Gibbs free energy and enthalpy of reaction, **Figure 8**, shows that at $T > 6273 \text{ K}$, there is an inflexion point for the Gibbs free energy to a negative ΔG making the reaction thermodynamically feasible in the plasma reactor. For temperatures above 6273 K , an increase in the temperature of the thermal plasma reactor leads to an increase in the magnitude of the Gibbs free energy indicating that this reaction is more favourable at high-temperature conditions. Also, the enthalpy of the reaction is >0 (across the entire temperature range) implying the reaction is endothermic and requires thermal energy to be driven towards equilibrium. At such high temperatures, it is expected that all species exist in the gaseous phase thereby requiring a quenching system to generate solid particles from gaseous metals.

3.4 Effect of pressure

The proposed 3CLAP process at atmospheric pressure has several advantages:

1. there is no complexity associated with maintaining the pressure and temperature of each reactor. Since pressure and temperature can have a synergic or non-synergic effect on the performance of the reactors (e.g., nitridation and ammoniation), the operation of the reactors at atmospheric pressure can minimise the complexity and technical challenges due to the temperature–pressure interaction in the reactors.

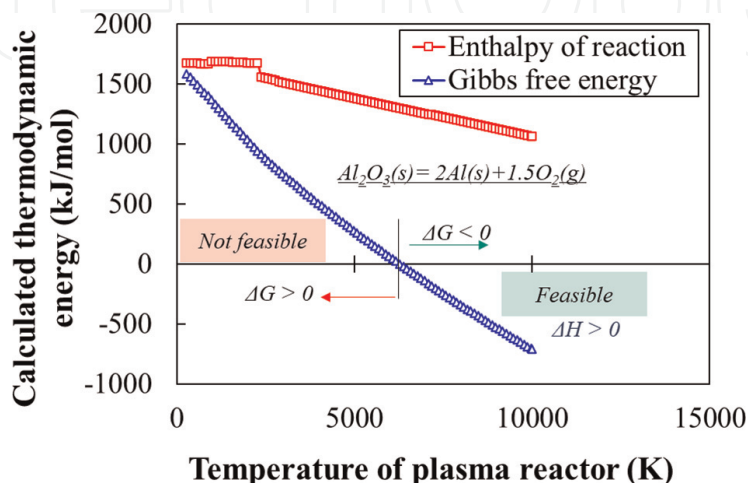


Figure 8. Variation of the Gibbs free energy and enthalpy of reaction with the temperature inside the thermal plasma reactor.

2. Thermal plasma reactor [43] is a relatively new technology, and most reactors operate at atmospheric or slightly positive pressure conditions. Hence, it is technically challenging to pressurise a thermal plasma reactor that has internal delicate electrodes, narrow gaps, and thin walls.
3. Operations at high-pressure, high-temperature conditions [44, 45] create a harsh environment that requires specific design, construction materials (e.g., Inconel, fortified steel with passive protection, or carbon fibre). This strongly affects the economic viability of the process and weakens the justifications and techno-economic aspects of the plant. Hence, pressurising the reactors should be avoided as much as technically possible to reduce the Levelized Cost of Energy (LCOE) in the proposed system.

3.5 Thermodynamic characterisation of the process

The performance of the system based on the 1st law efficiency, nitrogen economy, steam consumption, exergy partitioning factor and self-sustaining factor are depicted in **Figure 9**. As can be seen, the 3CLAP process transport exergy in form of chemical exergy by partitioning it in hydrogen and ammonia as the main products of the system. Hence, a parameter is defined as Exergy Partitioning Factor to account for the fraction of energy that is partitioned in the ammonia and hydrogen. Additionally, using a heat recovery system, the energy recovered from outlet products and streams are recovered and converted into steam to produce electricity for supplying the energy demanded by the thermal plasma reactor. Hence, a parameter is defined as the Self-Sustaining Factor (SSF) defined as the ratio of electricity produced by the heat recovery block to the energy demand of the thermal plasma reactor. The results showed that the designed process can achieve an SSF value of ~ 0.11 without incorporating renewable energy or external energy resources.

Also, it was found that the nitrogen and steam economy of the process is >1.8 and < 1 showing that the proposed system can deliver 1 mol of ammonia at cost of

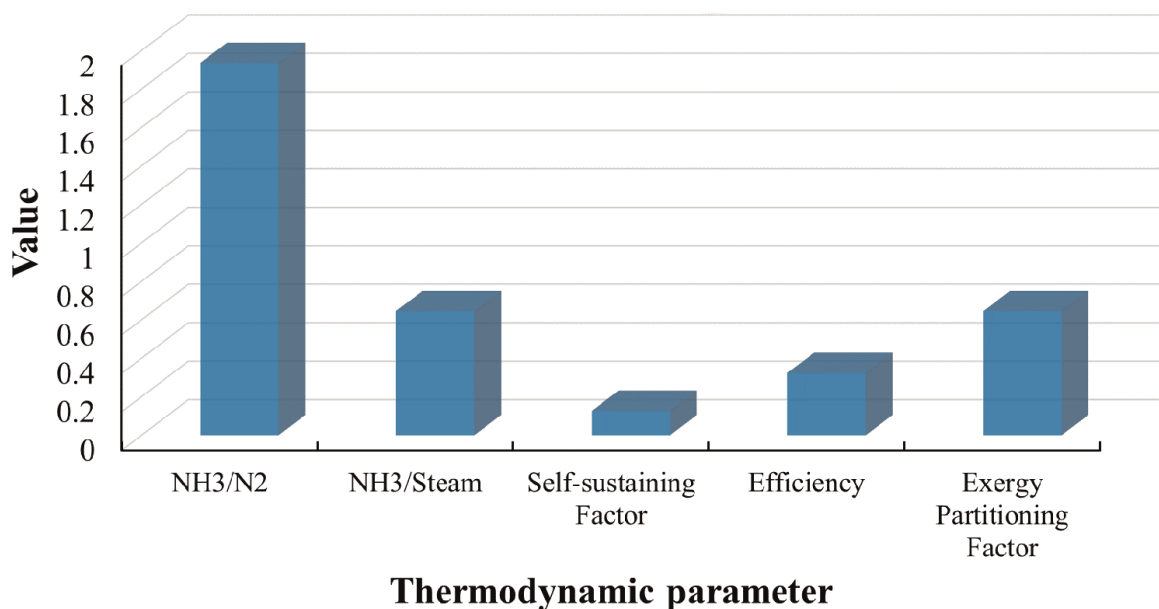


Figure 9. The effect of the temperature of the thermal plasma reactor on self-sustaining and exergy partitioning factors.

consuming ~ 2 mol of nitrogen and < 1 mol of steam. Since steam production costs vary depending on the source of water, the proposed system can offer a plausible Levelized Cost of Energy and techno-economic value for ammonia production. Notably, to produce ammonia, the temperature of the ammoniation reactor should be as low as 300 K to promote the economic viability aspects of the ammoniation reactor.

3.6 Renewable energy penetration - integration with solar energy

In this section, an example of hybridisation of the 3CLAP with solar photovoltaic energy is represented to calculate the solar share and to obtain the installation capacity required for the PV panel. It further elaborates on which fraction of solar energy can penetrate the system, thereby reducing the CO₂ emission from the plant. While the entire thermodynamic plant is a zero-carbon process, energy demands for the reactors can contribute greenhouse gases to the environment. Thus, it is critical to demonstrate how the proposed process can operate with renewable energy. **Figure 10** represents the frequency of energy demand (**Figure 10a**) and its diurnal/annual fluctuations (**Figure 10b**) from the plant calculated for a case study to produce ~ 1 tonne/day of ammonia. The energy algorithm of the plant was defined such that using renewable energy and energy produced by the built-in power cycle are prioritised. However, if both sources cannot meet the demand of the process, the energy from the grid is ramped up to meet the demand.

A 2.1 MW generator was calculated for the grid network to adapt to demand fluctuations. Considering a chain of 4 kW DC to AC converters, the performance of the system for a location at Geelong, Victoria in Australia (where solar reception is moderate) was evaluated. As can be seen, the solar share increases with an increase in the PV installation capacity reaching 28.4% at PV installation capacity of ~ 5 MW and 33.6% at installation capacity of 10 MW. Notably, the solar share can be improved by adding battery storage units to the system to address the intermittent behaviour of solar irradiance. However, a detailed assessment of renewable energy penetration is not part of the main goal of this study.

4. Outlook and future of the technology

The proposed technology in this chapter offered the potential to co-produce ammonia and hydrogen via a built-in heat recovery system and photovoltaic solar energy.

The thermodynamic models developed in this chapter assessed the energetic performance of the process and identified the thermodynamic limitations associated with the use of a thermal plasma reactor. The optimum operating temperature, and feed conditions together with the phase stability diagram for the aluminium particles in the thermal plasma reactor were obtained via equilibrium chemical analysis based on the Gibbs minimisation method. The results of this study showed that:

1. From the thermodynamic aspect, the process is feasible, with plausible efficiency and exergy partitioning fraction, thereby, there is no thermodynamic barrier avoiding the operation of this cyclic process.
2. The thermodynamic potential of the system for integrating with renewable energy resources, such as photovoltaic solar energy, highlighted that the

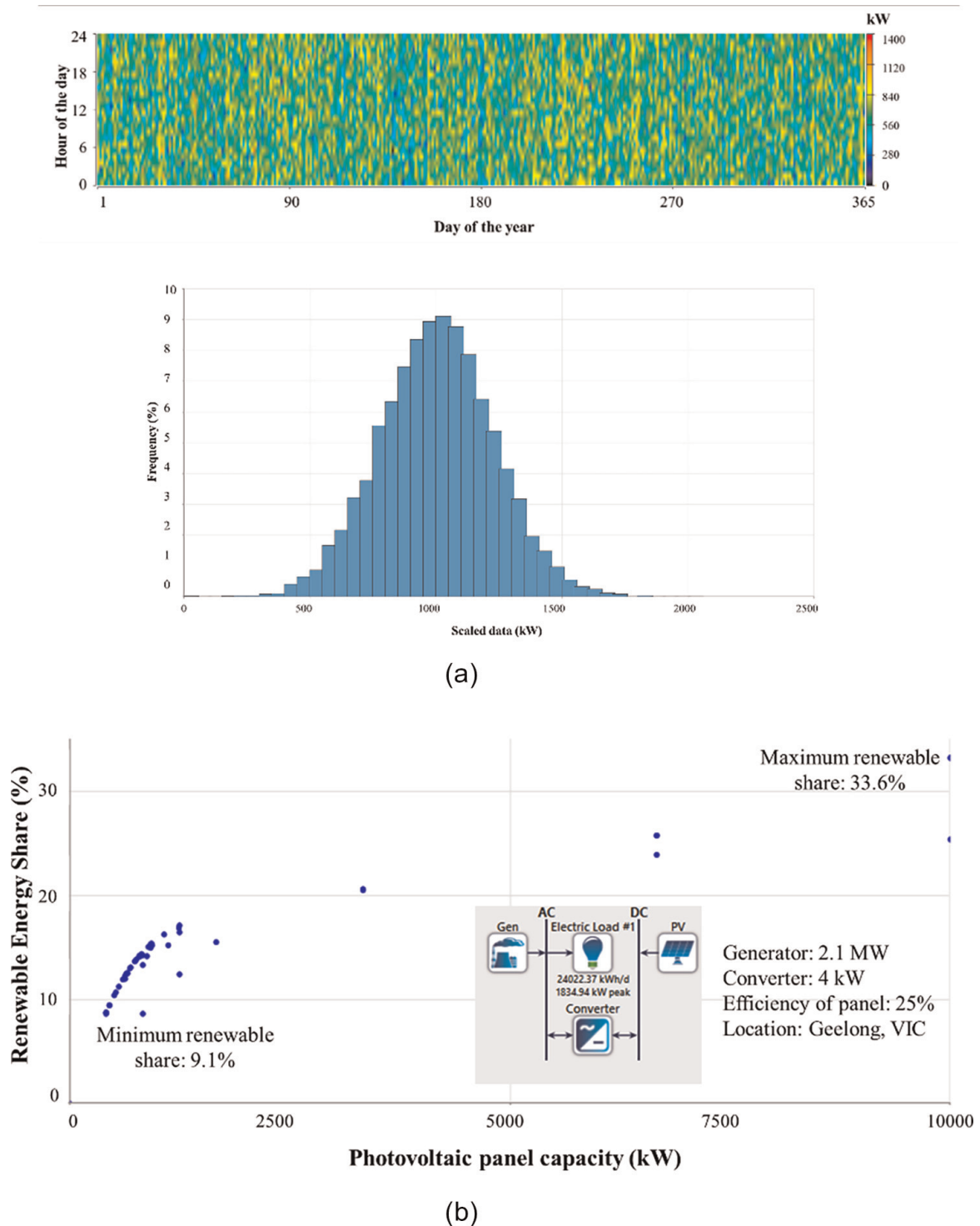


Figure 10. (a) Scattering and distribution of the process plant dynamic energy demand data calculated with Aspen plus, (b) the calculated renewable energy fraction of the system based on the diurnal solar radiance profile obtained in Geelong, Victoria 3220.

proposed process is resilient when using renewable energy for either small-scale or large-scale production of ammonia and hydrogen. For example, at 1 tonne/day production, an instant solar share (share of renewable energy without any storage units) ranged from 21% to 33.6%. It means that by considering SSF = 10%, about 43% of the demand can be maintained by the renewable energy resource and heat recovery from the products.

3. The proposed process can have various industrial applications. For example, in a centralised mode, it can be integrated with an air separation unit (ASU). The ASU generates oxygen from the air and the side product of the plant is nitrogen (or vitiated air which has reduced oxygen). While oxygen is produced from both ASU and 3CLAP, the nitrogen from ASU can be fed in the proposed process to be converted to ammonia for fertiliser production. Also, the proposed process can be integrated with gas-cooled power plants (e.g., nuclear) not only to utilise the nitrogen from the cooling loop, but also to generate electricity for the thermal plasma and also to be injected into the grid. The other application of the proposed system is to be utilised in areas where solar reception is high. While a thermal plasma reactor can be built in any area with good solar reception, the rest of the plant can be developed next to water resources (for steam generation) and near nitrogen down streams. Hence, the proposed process can be designed in a de-centralised (localised) mode.

While the feasibility of the process was successfully demonstrated in this chapter, further studies are still required to promote the technology readiness level of the 3CLAP. The required studies are listed as follows:

4.1 Rapid quenching technology

To handle gas–solid reactions in a thermal plasma reactor, a rapid quenching system is required to be fabricated to quench the aluminium particles once formed in the plasma reactor. The quenching process reduces the Gibbs's free energy and hinders the particles from participating in the unwanted and side reactions with the oxygen and radicals adjacent to the external surface of the aluminium particles. While the feasibility of the carbon black formation with thermal plasma has already been demonstrated in the literature, further studies are required to fortify the technology for solid particle formation. The rapid quenching process must have a small residence time and a very high heat transfer coefficient for high heat flux removal capacity.

4.2 Thermo-kinetics behaviour of the reactions

This study demonstrated the process feasibility of the 3CLAP process using equilibrium thermodynamics assuming all reactions were to proceed to the equilibrium state. The developed models are accurate for nitridation, ammoniation and for thermal plasma reactor (as it operates at high temperatures). However, there are possibilities that reactions are terminated at a point away from equilibrium. For example, the presence of impurities, localised temperature gradient, and changes in the morphology and structure of the aluminium particles can affect the cyclic behaviour of the process and suppress the chemical performance of the system. Therefore, there is a need to further study the thermo-kinetics behaviour of the aluminium particles and develop general kinetics models for the reactions in each reactor.

4.3 Material selection and design

Thermal plasma is a new disruptive technology, recently demonstrated in the lab-scale and pilot-scale studies [46]. Therefore, there is still a need to conduct further studies on the type of materials that can be used for constructing the reactor, electrodes, pipes and joints. While the temperature of the plasma reactor can locally reach

10,000 K [47], the bulk gas can reach a temperature up to 2000-3000 K. This requires a comprehensive study on material constraint and a material selection considering erosion, corrosion, and transient studies aiming at measuring tear and wear occurring inside the plasma reactor.

4.4 Prototyping the reactors

To the best of the authors' knowledge, this process is novel and there is no processing plant fabricated or constructed for ammonia/hydrogen production via thermal plasma plant. Hence, once kinetics studies are conducted, with the knowledge developed during material selection and design, prototypes can be constructed to measure the real-time efficiency, and performance of the 3CLAP process. In addition, there is further potential for other metals to be utilised in the process, thereby blending aluminium with other metals is another viable option to improve the real-life performance of the reactors.

5. Conclusions

In this book chapter, the potential of co-production of ammonia and hydrogen via a thermal plasma-assisted chemical looping technology was investigated. The proposed system was hybridised with solar energy (photovoltaic) and the renewable energy share was calculated. The Following conclusions were also made:

1. The Gibbs free energy calculations showed that all reactions in the nitridation, ammoniation and thermal plasma reactor are thermodynamically feasible with $\Delta G = 579.1$ kJ/mol, $\Delta G = 321.8$ kJ/mol and $\Delta G = -16.4$ kJ/mol, respectively. In the nitridation and ammoniation reactors, both reactions were spontaneous and both reactors could operate at $T < 1000$ K to exclude any phase change phenomenon inside the reactor.
2. A thermal plasma reactor was successfully demonstrated to dissociate Al_2O_3 to reduced aluminium particles at $T > 6273$ K with Al and Al_2O_3 as stable thermodynamic phases at 6273 K $< T < 10,000$ K. At $T < 6273$ K, $\Delta G > 0$ resulting causes reactions to be infeasible.
3. The Self-Sustaining Factor (SSF) and Exergy Partitioning Fraction (EPF) were calculated based on the energy demand of the thermal plasma and lower heating value (LHV) partitioned in the products, respective. It was identified that while the efficiency of the plant is $>32\%$, the SSF and EPF are 0.11 and 0.65, respectively showing that the system can supply 11% of its energy using steam combined heat recovery and the exergy transported to the ammonia/hydrogen stream is 65%.
4. At a production capacity of 1 tonne/day (NH_3 basis), the integration of the 3CLAP with photovoltaic solar (with PV installation capacity of 3 MW up to 10 MW) showed that the instant renewable energy share can be as high as 21% to 33.6%, respectively (without using battery storage unit) which can be improved by adding battery storage or further integration with wind energy.

Overall, the thermodynamic assessments revealed that the 3CLAP system is considered as one of the processes for green ammonia and hydrogen production. However, its configuration can vary depending on the end-user requirements and geographical needs.

Acknowledgements

Dr. Mohsen Sarafraz gratefully acknowledges the financial support and research funding “PRESS 2022” received from Deakin University. Dr. Mohsen Sarafraz acknowledges the financial support received via the “Alfred Deakin Postdoctoral Research Fellowship”.

Conflict of interest

The authors declare no conflict of interest.

Dedication

This book chapter is dedicated to the loving memory of my late mother, Fatemeh Sarraf, an angel whom I lost due to the COVID-19 outbreak in 2021. Also, it is dedicated to my beloved wife who supported me during the ups and downs of my life journey.

Author details


Mohsen Sarafraz^{1*}, Farid Christo² and Bernard Rolfe¹

1 School of Engineering, Deakin University, Geelong, Victoria, Australia

2 School of Aerospace Engineering and Aviation, RMIT University, Australia

*Address all correspondence to: mohsen.sarafraz@deakin.edu.au

IntechOpen

© 2022 The Author(s). Licensee IntechOpen. This chapter is distributed under the terms of the Creative Commons Attribution License (<http://creativecommons.org/licenses/by/3.0>), which permits unrestricted use, distribution, and reproduction in any medium, provided the original work is properly cited. 

References

- [1] Kandemir T, Schuster ME, Senyshyn A, Behrens M, Schlögl R. The Haber–Bosch process revisited: On the real structure and stability of “ammonia iron” under working conditions. *Angewandte Chemie International Edition*. 2013;**52**:12723-12726
- [2] Erisman JW, Sutton MA, Galloway J, Klimont Z, Winiwarter W. How a century of ammonia synthesis changed the world. *Nature Geoscience*. 2008;**1**: 636-639
- [3] Leigh GJ. Haber-bosch and other industrial processes. In: *Catalysts for Nitrogen Fixation*. Dordrecht: Springer; 2004. pp. 33-54
- [4] Moradi M, Ghorbani B, Ebrahimi A, Ziabasharhagh M. Process integration, energy and exergy analyses of a novel integrated system for cogeneration of liquid ammonia and power using liquefied natural gas regasification, CO₂ capture unit and solar dish collectors. *Journal of Environmental Chemical Engineering*. 2021;**9**:106374
- [5] Smith C, Hilla AK, Torrente-Murcianob L. Current and future role of Haber-Bosch ammonia in a carbon-free energy landscape. *Energy & Environmental Science*. 2020;**13**(2): 331-344
- [6] Zheng J, Jiang L, Lyu Y, Jian SP, Wang S. Green synthesis of nitrogen-to-Ammonia fixation: Past, present, and future. *Energy & Environmental Materials*. 2021;1-6. DOI: 10.1002/eem2.12192
- [7] MacFarlane DR, Cherepanov PV, Choi J, Suryanto BHR, Hodgetts RY, Bakker JM, et al. A roadmap to the ammonia economy. *Joule*. 2020;**4**: 1186-1205
- [8] Luo M, Yi Y, Wang S, Wang Z, Du M, Pan J, et al. Review of hydrogen production using chemical-looping technology. *Renewable and Sustainable Energy Reviews*. 2018;**81**:3186-3214
- [9] Kang K-S, Kim C-H, Bae K-K, Cho W-C, Kim S-H, Park C-S. Oxygen-carrier selection and thermal analysis of the chemical-looping process for hydrogen production. *International Journal of Hydrogen Energy*. 2010;**35**: 12246-12254
- [10] Li F, Kim HR, Sridhar D, Wang F, Zeng L, Chen J, et al. Syngas chemical looping gasification process: Oxygen carrier particle selection and performance. *Energy & Fuels*. 2009;**23**: 4182-4189
- [11] Adánez J, de Diego LF, García-Labiano F, Gayán P, Abad A, Palacios JM. Selection of oxygen carriers for chemical-looping combustion. *Energy & Fuels*. 2004;**18**:371-377
- [12] Brown TA, Scala F, Scott SA, Dennis JS, Salatino P. The attrition behaviour of oxygen-carriers under inert and reacting conditions. *Chemical Engineering Science*. 2012;**71**:449-467
- [13] Liu D-M, Tuan WH, Chiu C-C. Thermal diffusivity, heat capacity and thermal conductivity in Al₂O₃· Ni composite. *Materials Science and Engineering: B*. 1995;**31**:287-291
- [14] Xing C, Li M, Fu Y, Chen X, Lu P, Li X, et al. Improving thermal diffusivity of supported Fe-based Fischer–Tropsch catalysts to enhance long-chain hydrocarbon production. *Reaction Chemistry & Engineering*. 2021;**6**: 1230-1237

- [15] Ryu H-J, Kim J-W, Jo W-K, Park M-H. Selection of the best oxygen carrier particle for syngas Fueled chemical-looping combustor. *Korean Chemical Engineering Research*. 2007; **45**:506-514
- [16] Abuelgasim S, Wang W, Abdalazeez A. A brief review for chemical looping combustion as a promising CO₂ capture technology: Fundamentals and progress. *Science of the Total Environment*. 2021;**764**: 142892
- [17] He Z, De Wilde J. Numerical simulation of commercial scale autothermal chemical looping reforming and bi-reforming for syngas production. *Chemical Engineering Journal*. 2021;**417**: 128088
- [18] Nguyen NM, Alobaid F, Dieringer P, Epple B. Biomass-based chemical looping gasification: Overview and recent developments. *Applied Sciences*. 2021;**11**:7069
- [19] Sarafray MM, Christo FC. Sustainable three-stage chemical looping ammonia production (3CLAP) process. *Energy Conversion and Management*. 2021;**229**:113735
- [20] Udomsirichakorn J, Salam PA. Review of hydrogen-enriched gas production from steam gasification of biomass: The prospect of CaO-based chemical looping gasification. *Renewable and Sustainable Energy Reviews*. 2014; **30**:565-579
- [21] Sun H, Wang Z, Fang Y, Liu Z, Dong L, Zhou X, et al. A novel system of biomass for the generation of inherently separated syngas by combining chemical looping CO₂-gasification and steam reforming process. *Energy Conversion and Management*. 2022;**251**:114876
- [22] Xu J, Song T. CO₂-gasification kinetics of biomass char with a red mud oxygen carrier for chemical looping combustion. *Fuel*. 2022;**313**:123011
- [23] He S, Gao L, Dong R, Li S. A novel hydrogen production system based on the three-step coal gasification technology thermally coupled with the chemical looping combustion process. *International Journal of Hydrogen Energy*. 2022;**47**:7100-7112
- [24] Pan Q, Ma L, Du W, Yang J, Ao R, Yin X, et al. Hydrogen-enriched syngas production by lignite chemical looping gasification with composite oxygen carriers of phosphogypsum and steel slag. *Energy*. 2022;**241**:122927
- [25] Bale CW, Chartrand P, Degterov SA, Eriksson G, Hack K, Mahfoud RB, et al. FactSage thermochemical software and databases. *Calphad*. 2002;**26**: 189-228
- [26] Zhao K, Fang X, Huang Z, Wei G, Zheng A, Zhao Z. Hydrogen-rich syngas production from chemical looping gasification of lignite by using NiFe₂O₄ and CuFe₂O₄ as oxygen carriers. *Fuel*. 2021;**303**:121269
- [27] Dry ME. The fischer-tropsch process: 1950–2000. *Catalysis Today*. 2002;**71**:227-241
- [28] Dry ME, Hoogendoorn JC. Technology of the Fischer-Tropsch process. *Catalysis Reviews—Science and Engineering*. 1981;**23**:265-278
- [29] Zhang H-F, Chen L, Liu X-Y, Ge H-J, Song T, Shen L-H. Characteristics of cyanobacteria pyrolysis and gasification during chemical looping process with red mud oxygen carrier. *Journal of Fuel*

Chemistry and Technology. 2021;**49**:
1802-1810

[30] Givler T, Lilienthal P. Using HOMER Software, NREL's Micropower Optimization Model, to Explore the Role of Gen-Sets in Small Solar Power Systems; Case Study: Sri Lanka. Golden, CO (US): National Renewable Energy Lab; 2005

[31] Kangas P, Hannula I, Koukkari P, Hupa M. Modelling super-equilibrium in biomass gasification with the constrained Gibbs energy method. *Fuel*. 2014;**129**:86-94

[32] Koukkari P, Pajarre R, Hack K. Constrained Gibbs energy minimisation. *International Journal of Materials Research*. 2007;**98**:926-934

[33] Yahom A, Powell J, Pavarajarn V, Onbhuddha P, Charojrochkul S, Assabumrungrat S. Simulation and thermodynamic analysis of chemical looping reforming and CO₂ enhanced chemical looping reforming. *Chemical Engineering Research and Design*. 2014;**92**:2575-2583

[34] Melgar A, Pérez JF, Laget H, Horillo A. Thermochemical equilibrium modelling of a gasifying process. *Energy Conversion and Management*. 2007;**48**: 59-67

[35] Barin I, Platzki G. Thermochemical Data of Pure Substances. Weinheim, VCh: Wiley Online Library; 1989

[36] Fulcheri L, Schwob Y. From methane to hydrogen, carbon black and water. *International Journal of Hydrogen Energy*. 1995;**20**:197-202

[37] Mostaghimi-Tehrani J, Pfender E. Effects of metallic vapor on the

properties of an argon arc plasma. *Plasma Chemistry and Plasma Processing*. 1984;**4**:129-139

[38] Donaldson A, Cordes RA. Rapid plasma quenching for the production of ultrafine metal and ceramic powders. *JOM*. 2005;**57**:58-63

[39] Wang X, Su M, Zhao H. Process design and exergy cost analysis of a chemical looping ammonia generation system using AlN/Al₂O₃ as a nitrogen carrier. *Energy*. 2021;**230**:120767

[40] Kalogirou S. Recent patents in absorption cooling systems, recent patents on. *Mechanical Engineering*. 2008;**1**:58-64

[41] Maarefian M, Bandehali S, Azami S, Sanaeepur H, Moghadassi A. Hydrogen recovery from ammonia purge gas by a membrane separator: A simulation study. *International Journal of Energy Research*. 2019;**43**:8217-8229

[42] Gálvez ME, Halmann M, Steinfeld A. Ammonia production via a two-step Al₂O₃/AlN thermochemical cycle. 1. Thermodynamic, environmental, and economic analyses. *Industrial & Engineering Chemistry Research*. 2007;**46**:2042-2046

[43] Taylor PR, Pirzada SA. Thermal plasma processing of materials: A review. *Advanced Performance Materials*. 1994;**1**:35-50

[44] Min JK, Jeong JH, Ha MY, Kim KS. High temperature heat exchanger studies for applications to gas turbines. *Heat and Mass Transfer*. 2009;**46**:175-186

[45] Ho CK, Carlson M, Albrecht KJ, Ma Z, Jeter S, Nguyen CM. Evaluation of alternative designs for a high

temperature particle-to-SCO₂ heat exchanger. American Society of Mechanical Engineers. 2019;**141**: V001T011A007

[46] Gomez E, Rani DA, Cheeseman CR, Deegan D, Wise M, Boccaccini AR. Thermal plasma technology for the treatment of wastes: A critical review. *Journal of Hazardous Materials*. 2009; **161**:614-626

[47] Mishin J, Vardelle M, Lesinski J, Fauchais P. Two-colour pyrometer for the statistical measurement of the surface temperature of particles under thermal plasma conditions. *Journal of Physics E: Scientific Instruments*. 1987; **20**:620